JOURNAL OF SPACECRAFT AND ROCKETS
Vol. 43, No. 2, March–April 2006

Entry Vehicle Control System Design for the Mars Science Laboratory

Philip C. Calhoun* and Eric M. Queen*
NASA Langley Research Center, Hampton, Virginia 23681

The NASA Langley Research Center, in cooperation with the Jet Propulsion Laboratorty, participated in a preliminary design study of the entry, descent, and landing phase for the Mars Science Laboratory Project. This project uses advances in guidance, navigation, and control technology to significantly improve Mars surface targeting capability. A candidate entry controller based on the reaction control system controller for the Apollo command module digital autopilot is proposed for use in the entry attitude control. Modifications to the phase plane controller provide good bank-angle response, reduce jet-firing chattering for hogh-frequency updates, and allow for the option of aerodynamic angle feedback for the Martian entry probe application. The controller performance is demonstrated in a six-degrees-of-freedom simulation with representative aerodynamics.

Nomenclature

I	=	moment of inertia
M_θ	=	derivative of moment with respect to angle
p	=	body-axis roll rate
q	=	body-axis pitch rate
r	=	body-axis yaw rate
α	=	angle of attack
α_{RCS}	=	angular acceleration from reaction control system
θ_C	=	angle offset of center of elliptical trajectory
θ_{DB}	=	angle deadband
θ_E	=	angle error
θ_S	=	angle shift within phase plane because of error in trim
ω_{SP}	=	short-period mode frequency

Subscript

trim	=	trim condition

Introduction

THE NASA Langley Research Center, in cooperation with the Jet Propulsion Laboratory, participated in a preliminary design study of the entry, descent, and landing phase for the Mars Science Laboratory (MSL) Project. This concept utilizes advances in guidance, navigation, and control technology to significantly improve Mars surface targeting capability, allowing scientific missions to specific surface features. This paper documents a candidate entry vehicle controller design for the MSL project. The entry vehicle has a conical forebody and a truncated biconical aft body as shown in Fig. 1. The entry phase of flight begins at the atmospheric interface and ends at the supersonic parachute deployment.

A second control system is required for the powered descent phase after the lander is released from the parachute; only the entry phase of flight is addressed in this paper. During atmospheric entry, the vehicle is flown with its axis of symmetry at an angle to the relative velocity direction (angle of attack). The airflow over the vehicle produces a lift force normal to the velocity vector. Orientation of the lift vector, via bank-angle steering, allows the guidance system to maneuver the vehicle to the targeted parachute deployment conditions (i.e., latitude and longitude). The controller objective is to maintain the entry vehicle angle of attack, bank angle, and sideslip angle, at the commanded values to within specified tolerances. The angle of attack is commanded to follow the predicted pitch trim values across the Mach range. To accomplish coordinated bank maneuvers, the sideslip angle is commanded to zero during the entry phase. Eight reaction control system (RCS) thrusters mounted in pairs at four locations, as shown in Fig. 1, achieve control actuation.

Two methods were considered to maintain pitch torque equilibrium for MSL flight at a fixed angle of attack: 1) a radial c.g. offset and 2) an aerodynamic trim surface, either fixed or deployed. The c.g. offset option was chosen as the project baseline due to design heritage, and the controller design was developed for this configuration. To be consistent with the coordinate system conventions shown in Fig. 1, the radial c.g. offset is located along the $-Z_B$ coordinate direction. Because the vehicle is axisymmetric, the c.g. offset configuration has no significant roll stiffness or roll damping for small deviations from trim conditions; therefore, the lateral and directional axes are assumed to be decoupled for the purpose of controller design. This allows for a single-axis control design methodology for each of the pitch, yaw, and roll axes. The phase-plane method is well suited for control design using on/off actuation devices with little interaction between the axes; therefore, a phase-plane controller for each axis was chosen as a candidate approach.[1]

During the entry phase, bank-angle modulation is used to drive the vehicle to the target parachute deploy point. Reversals of 180 deg or more can be commanded to adjust the nominal trajectory downrange and crossrange. The flight mechanics team, using the Program for the Optimization of Simulated Trajectories analysis tool, provided flight conditions for a typical entry.[2] Nominal values of angle of attack and dynamic pressure for a typical entry trajectory are shown in Fig. 2.

The entry flight control system will utilize RCS jets to control and stabilize the vehicle attitude during the entry phase of flight. The controller design is based on the RCS controller for the Apollo command module (CM) digital autopilot.[3] The CM RCS controller used a phase-plane technique that provided a compromise between maneuver time and fuel usage.[3] The phase plane is defined as a plot of rate error vs position error. The control approach is based on selection of on/off RCS firing commands, determined by location of the states relative to switching curves in the phase plane.

Because the RCS system has a finite minimum impulse, the system will not, in general, be able to reach the commanded state exactly. One of the challenges of developing a controller for this type of system is to bring the terminal condition close to the commanded condition with minimal overshoot during large angle maneuvers. Additionally, when the error is large, the control system should respond with full control effort. For the MSL application, the guidance

Presented as Paper 2002-4504 at the AIAA Atmospheric Flight Mechanics Conference, Monterey, CA, 5–8 August 2002; received 20 February 2003; revision received 1 August 2004; accepted for publication 1 February 2005.

*Research Engineer. Member AIAA.

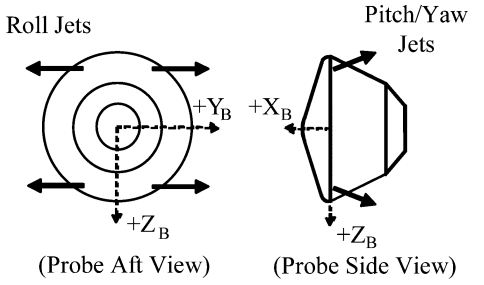

Fig. 1 Reaction control system layout.

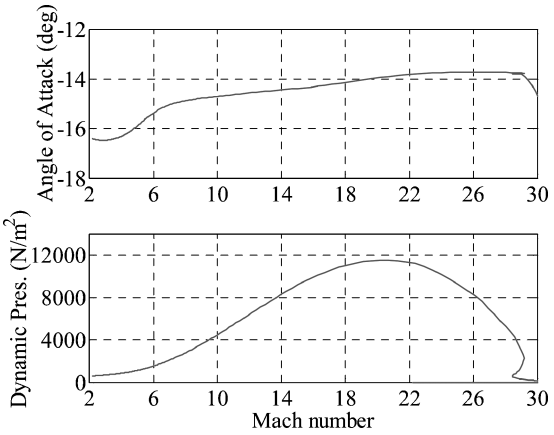

Fig. 2 Nominal entry trajectory.

system requires a minimum bank acceleration of 5 deg/s^2 and bank reversal rate of 20 deg/s to achieve the desired targeting capability.[4] This requirement, and the moments of inertia of the vehicle, drive the thruster size of the RCS.

Performance of the candidate RCS control law was analyzed using a nonlinear six-degree-of-freedom (DOF) simulation of typical flight conditions. The results included dynamic responses to representative guidance commands and estimates of RCS firings and fuel usage. The six-DOF simulation included the Mars Global Reference Atmospheric Model 2000,[5] as well as a simplified gravity model including the J2 perturbation from a spherical field. This flight simulation was written using the Simulink™(Ref. 6) toolbox in MATLAB™.[7]

Model Descriptions

Aerodynamics

The entry vehicle aerodynamic database used for the MSL entry controls design and analysis was developed at NASA Langley Research Center.[8] It is based on computational-fluid-dynamics calculations and wind-tunnel measurements. The database, originally developed for the Mars 2001 Lander, includes six-DOF force and moment coefficients from noncontinuum flow conditions through hypersonic flight down to Mach 1.4 with total angle of attack ranging from 0 to 16 deg. The database was extrapolated at low supersonic Mach numbers for angle of attack up to 19 deg to accommodate the expected angle range for MSL. This database was used for the purposes of evaluating the controller design for the baseline axisymmetric configuration. An additional aerodynamic database for a nonaxisymmetric configuration, using an aerodynamic trim surface, was also developed for the MSL.[9] The MSL project chose not to pursue this configuration, and so this database was not used for control design and analysis.

RCS Configuration

The RCS jets used for entry control are located on the backshell near the maximum diameter as shown in Fig. 1. Currently, the MSL detailed design is not complete, and the final RCS configuration has not been selected. The configuration shown in Fig. 2 is representative of the baseline design and was used for the purpose of this study. Four nearly tangential jets are used to provide roll torques for bank-angle maneuvers. Four aft-firing jets, each coincidently located with a roll jet, provide pitch/yaw torques to control the vehicle angle of attack and to maintain zero sideslip for coordinated bank maneuvers. This configuration was chosen to provide roll control independent from yaw control, allowing adjustment of the roll/yaw control acceleration ratio over a range of angle of attack and vehicle inertia values. This is necessary to maintain zero sideslip during bank maneuvers. Independent control of pitch and yaw was unnecessary because of inherent pitch stability and few pitch firings anticipated. For the purpose of this initial controller evaluation, the RCS jets were modeled as perfect on/off devices with an instantaneous rise time, no internal lags, and no thrust decay. RCS commands are updated at a 50 Hz rate, which is consistent with the minimum on time for the baseline thrusters.

The four aft-firing thrusters cannot be commanded to provide independent pitch and yaw control. That is, if a command is given for pitching moment and yawing moment simultaneously, the thrusters cannot provide both at their full capability. Simultaneous pitch/yaw actuation results in jet firing on commands of diagonally offset thrusters. Firing diagonally opposing thrusters simultaneously results in no net moment, as seen from the RCS configuration in Fig. 1. Whenever this happens, the diagonally opposite pair of jet firing commands is ignored, and only the remaining jet firing is executed in the RCS. Thus, half control effort is executed for both pitch and yaw during this command period. Because the vehicle has good static pitch stability across the Mach range, few pitch-axis firings were noted in simulations studies. Vehicle closed-loop performance was not degraded noticeably during infrequent simultaneous pitch/yaw commands. Because the desired roll and yaw motions are tightly coupled during large bank maneuvers, independent control of the roll and yaw channels is considered more important than tight control of the pitch channel. With this in mind, alternate jet selection logic could be set to give the yaw channel priority over the pitch channel during simultaneous commands. However, this approach was not implemented because the baseline approach demonstrated good performance in the simulation studies.

Phase-Plane Controller

A phase-plane controller is based on behavior of the vehicle dynamics in the plane defined by state errors vs state rate errors. For instance, sideslip error vs sideslip rate error would define a phase plane in the directional channel of the vehicle. Experience has shown that the MSL entry attitude dynamics can be treated as a set of decoupled single-input, single-output systems as long as the pitch and yaw angular rates are kept small with moderate roll rates. The single-axis phase-plane controller approach performed well in the six-DOF simulation with roll rates as high as 20 deg/s during large angle maneuvers. A phase-plane controller is designed by selection of switching curves that define regions within the phase plane of on/off commands for each RCS channel. These switching curves are selected to drive the state error trajectory to the desired limit cycle, that is, to within a specified angle error deadband. Additionally, large angle maneuvers should be accomplished quickly with minimal command overshoot. Figure 3 shows a representative phase plane for the MSL roll axis and is used to illustrate this controller design approach in the following section.

The objective of the MSL controller was to track bank-angle commands from the guidance system while maintaining the vehicle attitude near the static trim conditions. Several modifications to the Apollo CM phase-plane approach were made to meet the MSL application requirements. The CM vehicle had ample static stability; thus, angle-of-attack and sideslip-angle feedback were not used for stability augmentation or performance of coordinated bank maneuvers.[3] An option for angle-of-attack and sideslip feedback was implemented in the MSL entry controller to improve trim angle tracking and/or assist bank coordination at low dynamic pressure conditions. The CM autopilot bank-angle commands were updated at 0.5 Hz, and rate feedback for the angle-of-attack and sideslip channels was executed at 10 Hz. The MSL precision control requirement for parachute-deploy targeting has driven the MSL entry guidance

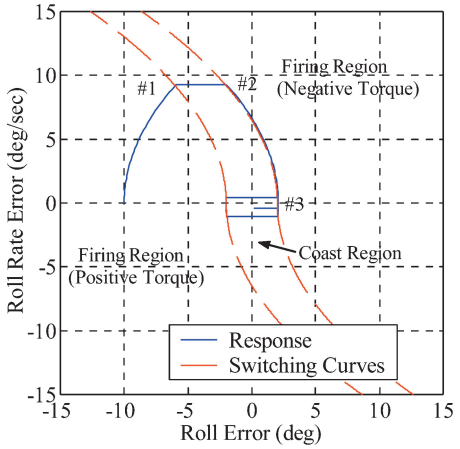

Fig. 3 Roll phase plane, initial condition response.

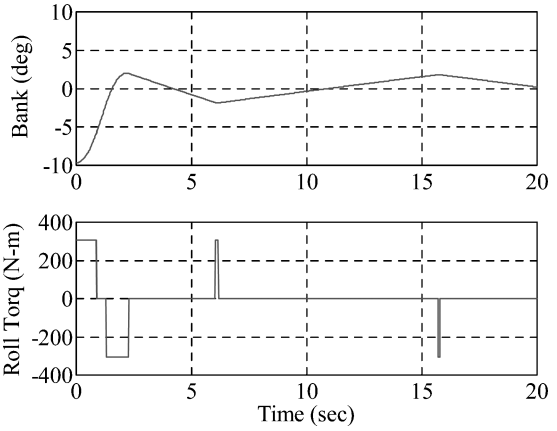

Fig. 4 Roll initial condition response.

update to 10 Hz. This resulted in a necessary increase in controller update rate. To improve targeting performance, rapid bank-angle response to command reversals was also considered desirable, even if it resulted in a fuel usage increase. Axis coupling caused by aerodynamics/RCS interaction was considered small and thus neglected in the Apollo CM autopilot design. An effort to predict the amount of axis coupling as a result of aerodynamics/RCS for the MSL configuration is ongoing. For the purpose of this MSL study, axis coupling will be neglected. The next two sections describe the specific controller modifications made to the roll and angle-of-attack/sideslip axes, respectively.

Roll-Axis Control

Modifications to the CM controller included changes to the roll-axis channel. First, to minimize guidance/control interaction the controller update rate was set at 50 Hz ensuring adequate frequency separation from the 10-Hz guidance update rate. A predictive phase-plane algorithm, as implemented for the CM roll axis, was not necessary for the MSL application because the controller update rate was near the minimum firing duration of the RCS thrusters.[3] Instead, the instantaneous estimated states determine the phase-plane location and hence the RCS firing command, until the next controller update. The use of a control line to define the coast region lower boundary,[3] with slope equal to 0.25 in the CM phase plane, was replaced with a parabolic switching curve parallel to the original upper curve. This allowed the MSL bank response to be more rapid than for the CM. The modified roll phase plane is shown in Fig. 3.

The equation defining the switching curves in the phase plane is developed as follows. For small off-axis rotation rates gyroscopic coupling is not significant, and the roll axis can be treated as an independent double integrator over the guidance update interval. The resulting trajectory within the phase plane is parabolic during constant jet-on firing conditions. Thus, an appropriately defined parabolic curve, which terminates at a location within the phase plane near the origin, would define a set of suitable state conditions for switching on the RCS jets.[3] The curvature is determined by the jet-on angular acceleration, with terminus at a location of zero rate error and angle error of $\pm\theta_{\mathrm{DB}}$. Values of the angle error and the time derivative of angle error, which are solutions of Eq. (1) for both positive and negative values of RCS angular acceleration, define trajectories in the phase plane that bound regions of jet on/off firing conditions:

$$\theta_e = \pm\theta_{\mathrm{DB}} + (1/2\alpha_{\mathrm{RCS}})\dot{\theta}_e^2 \tag{1}$$

These curves, shown in Fig. 3, define boundaries within the phase-plane separating regions of jet-on firing commands in opposing roll directions from jet-off commands. These regions are called "firing" and "coast" regions, respectively.

A typical roll channel response, with an initial angle error of −10 deg and a roll command of zero, demonstrates the behavior of the modified CM phase-plane controller. The phase-plane plot with appropriately defined parabolic switching curves terminating at an angle deadband specification of ±2 deg is shown in Fig. 3. The roll error is defined as roll minus roll command, and the roll rate error is defined similarly. Initially the vehicle response lies in the firing region below the switching curves corresponding to a positive roll torque command. As the vehicle rate builds and the position error decreases, the vehicle follows the predicted parabolic path in the phase plane until the trajectory intersects the lower switching curve at location 1. The trajectory then enters the coast region between the lower and upper switching curve where the RCS command turns the roll jets off. Because the rate error is positive, the position error goes toward zero as the trajectory proceeds at constant rate from location 1 to 2. At this point, the trajectory crosses the upper switching curve and enters the firing region corresponding to negative RCS roll torque. Because the switching curves are defined as the second integral of roll acceleration, as described in Eq. (1), the trajectory within the phase plane follows the switching curve from location 2 to the desired location 3. At this point the roll response enters a limit cycle and thereafter remains within the roll deadband specification. Figure 4 shows the corresponding time-domain response and the associated roll torque from the RCS firings. In this example, the vehicle is commanded to zero from an initial roll of −10 deg.

This example demonstrates how the phase-plane controller can accomplish the task of driving the vehicle response within the desired deadband in reasonable time with minimal overshoot. The maneuver is completed, and the vehicle response enters the desired limit cycle with a single bang–bang torque doublet. The resulting optimal response is a tradeoff between fuel consumption and maneuver time for a given RCS angular acceleration.[3]

The roll channel responses in Figs. 3 and 4 demonstrate the performance of the modified CM phase-plane controller in the case of a constant set-point command. Consider the performance of this controller in response to a constantly changing tracking command, such as that from a realistic guidance command sequence.

Figure 5 shows the phase-plane response, and Fig. 6 shows the time-domain response, to a continuously varying chirp-type roll-angle command.

The roll angle follows the command reversals with minimal lag and acceptable overshoot at the end of the command sequence. However, the roll torque plot shows that the controller exhibits a high-frequency on/off cycling of the RCS jets known as "chattering." Because the command is varying, the dynamics of the error states within the phase plane no longer maintain the predicted parabolic shape during periods when the RCS jets are on. The resulting trajectories cross back and forth over the switching curves leading to the chattering response. This behavior is undesirable because it can lead to cyclic fatigue of the jet mechanisms and excessive fuel consumption. The Apollo CM used a predictive phase-plane approach with an update rate of 2 s, which avoided the problem of chattering.

To provide a design-flexible means of driving the state toward the desired deadband limit cycle, a slight modification was considered for coast region logic to eliminate the high-frequency chattering.

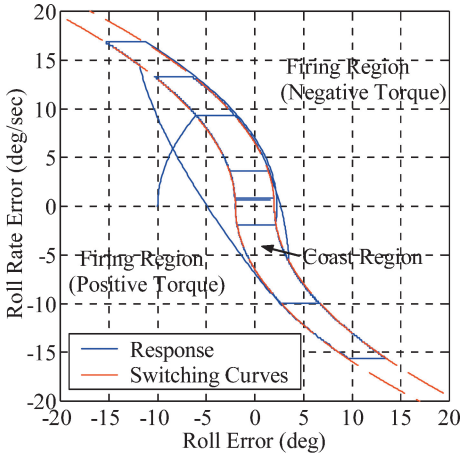

Fig. 5 Roll phase plane, "chirp" command response.

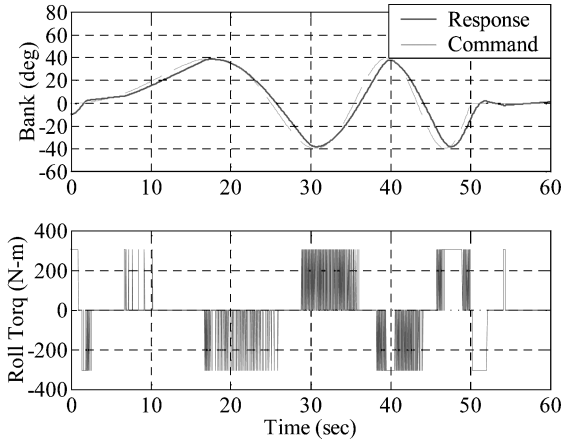

Fig. 6 Roll chirp command response.

Another set of switching curves was added to provide hysteresis in the on/off switching characteristics within the coast region. These additional curves were designed to provide good closed-loop performance while minimizing the chattering behavior of the RCS. The phase-plane switching curves also included a small delta in the switching curve termination location, as they approach zero rate error from the positive or negative directions. This forces the trajectory to enter the coast region as the rate error changes sign, which results in a minimum impulse jet firing limit cycle for periods of constant commands. Constant bank commands are typical guidance outputs at the beginning and end of the entry phase. Similar switching curve termination characteristics were utilized in the CM controller to achieve minimum impulse firing limit cycle.[3] The performance of the modified phase plane for the MSL roll axis is demonstrated in the Simulation Study section of this paper.

Angle-of-Attack and Sideslip-Angle Control

The CM controller used rate feedback only for the angle-of-attack and sideslip channels. Angle-of-attack rate was nominally estimated as the pitch rate in the CM controller. A flight-path angle rate correction was included near the end of the trajectory when the flight-path angle rate exceeded 0.5 deg/s. The effect of flight-path angle rate was neglected in the MSL control because, nominally, it does not exceed 0.5 deg/s. The CM controller enforced coordinated turns, that is, sideslip remaining near zero for a bank maneuver, by relying on static stability and by commanding the vehicle yaw rate as defined in Eq. (2):

$$r = p\tan(\alpha_{\text{trim}}) \tag{2}$$

This relation assumes that the angle-of-attack deviation from trim conditions and the pitch rate are negligible. To improve turn coordination and angle-of-attack tracking, particularly at low dynamic pressure, the MSL controller included aerodynamic angle feedback. This was implemented as a linear phase plane with an optional elliptical dead zone as shown in Fig. 7.

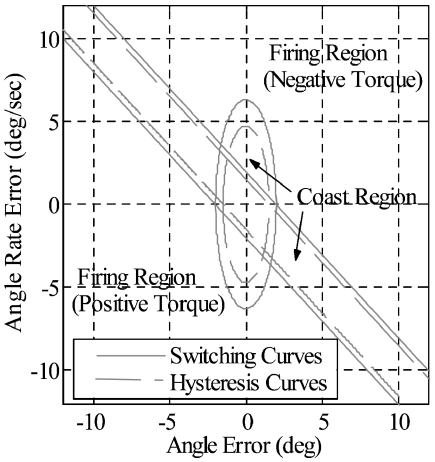

Fig. 7 Angle-of-attack and sideslip-angle phase plane.

The aerodynamic restoring moments are significant as the entry probe descends into the atmosphere; therefore, angle-of-atack and sideslip channels cannot be approximated as a double integrator. Neglecting aerodynamic damping, a simple harmonic oscillator serves as an approximate dynamics model for the statically stable plant. Values of the angle and the time derivative of the angle errors, which are real solutions of Eq. (3), define corresponding trajectories in the phase plane that cross through the point θ_{DB}:

$$\dot{\theta}_e = \omega_{\text{SP}}\left[\theta_{\text{DB}}^2 + 2\theta_c(\theta_{\text{DB}} - \theta_e) - \theta_e^2\right] \tag{3}$$

The resulting trajectories are elliptical, with centers located at values of θ_C, as defined in Eq. (4):

$$\theta_C = \alpha_{\text{RCS}} \big/ \omega_{\text{SP}}^2 \tag{4}$$

The semimajor axis of the ellipse is scaled by the short-period mode frequency ω_{SP}, which varies with flight condition. It is difficult to combine these elliptical trajectories to form an appropriate set of switching curves because they define overlapping closed regions within the phase plane for positive and negative values of RCS angular acceleration. Instead, a simple linear set of curves with negative slope serves to attract the phase-plane trajectory toward the origin. This can be determined by realizing that negative values of α_{RCS} and hence negative values of torque, result in shifting the phase-plane trajectory toward the negative angle values and vice versa. Thus, trajectories above the switching curves shown in Fig. 7 are in the negative firing region and migrate to the left, and trajectories below migrate right. After several cycles, the resulting trajectory is attracted toward the origin.

Another consideration is the choice of switching curve slope. If the slope is vertical, the resulting trajectory reaches a limit cycle and is not attracted toward the origin. A horizontal line is equivalent to the CM rate damper, which serves to drive the trajectory toward zero rate and hence toward the trim angle of attack. However, consider the case in which the probe does not trim at the expected angle of attack. This can occur if the aerodynamic pitching moment is mispredicted. This will result in a shift of the phase-plane trajectories by an amount θ_S, along the angle axis and away from the origin. Equation (5) gives the amount of this shift, as a function of the error in the trim angle and the derivative of moment with respect to the angle:

$$\theta_S = M_q \theta_{\text{E}_{\text{trim}}} \big/ I\omega_{\text{SP}}^2 \tag{5}$$

If the trim angle shift remains lower than θ_C, it is possible for the RCS to overcome this tendency for the steady-state trajectory to move away from the origin. However, this would require a switching curve with a nonzero slope. Furthermore, a switching curve with zero slope would allow the sideslip channel trajectory to drift away

from the command unacceptably during bank reversals at low dynamic pressure. On the other hand, at high dynamic pressure the aerodynamic restoring moment can exceed the ability of the RCS to overcome trim angle errors. In this condition angle control can result in excessive fuel consumption. Therefore, a variable slope with larger value during low dynamic pressure and near-zero value during maximum dynamic pressure can be a good design solution. This is analogous to decreasing the angle feedback as the dynamic pressure increases. A slope of -1 was chosen as a candidate for the MSL angle-of-attack and sideslip-angle channels. For this slope choice, six-DOF simulations demonstrated good performance with acceptable fuel usage for the expected range of aerodynamic moment uncertainty. Setting the switching curve slope to zero resulted in less fuel usage with a slight performance impact.

The addition of an elliptical coast region, as represented in Fig. 7, allows the vehicle to achieve higher angular rate values when the angle error is within the deadband specification. The elliptical shape of the coast region is a function of flight condition as defined by real solutions of Eq. (3) for zero values of RCS angular acceleration. This additional coast region allows the response to be tailored to flight condition. Implementing the linear curves as shown would result in an unnecessary reduction of the stabilized motion amplitude, particularly for conditions of high dynamic pressure. Thus, the addition of the elliptical coast region provides a potential for some fuel usage reduction.

The proposed phase-plane method for optional aerodynamic angle control requires some estimation of the aerodynamic angles from the navigation system. Ideally, the values of angle of attack, sideslip, and bank angle would be determined from the attitude relative to the relative wind velocity vector. The navigation system, as designed for MSL, provides a no-wind estimate of the attitude.[10] Combining inertial measurement units, with knowledge of the aerodynamic force and moment coefficients as a function of the estimated angles, could provide improved estimation capability. However, for the MSL application, six-DOF simulations have demonstrated adequate system performance for expected wind conditions using the navigated attitude for feedback.

Simulation Study

The modified CM phase plane controller was used for the MSL entry RCS controller, and the system performance was tested in a six-DOF simulation. A phase-plane controller utilizing linear switching curves with slope equal to -1 was used for the angle-of-attack and sideslip channels. The phase-plane controller with modified switching curves, described in the preceding section, was used for the roll axis. The simulated responses shown start near maximum dynamic pressure and continue to about Mach 3. The chirp-type command sequence, shown earlier, is used to demonstrate the control system performance.

The modified MSL roll phase plane, shown in Fig. 8, includes a set of hysteresis switching curves within the coast region of the phase plane.

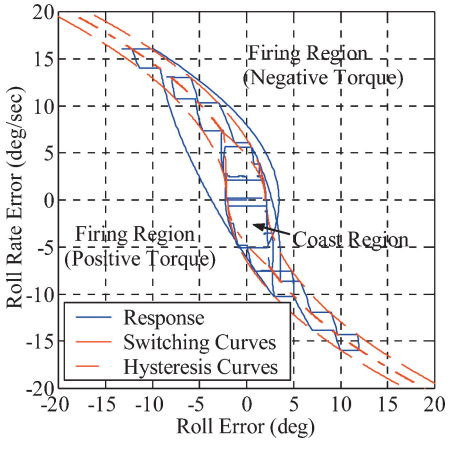

Fig. 8 Six-DOF case study, roll phase plane.

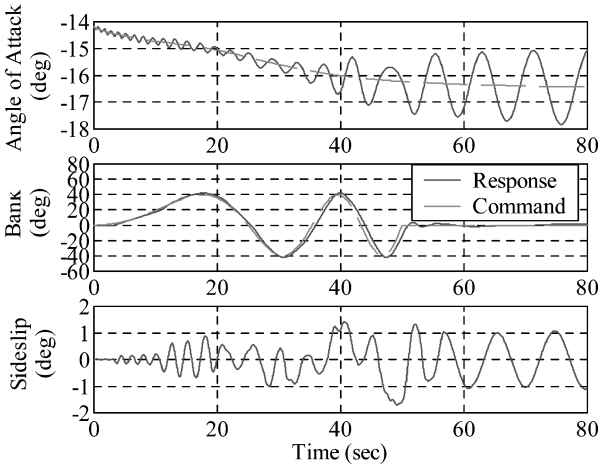

Fig. 9 Six-DOF case study, chirp command response.

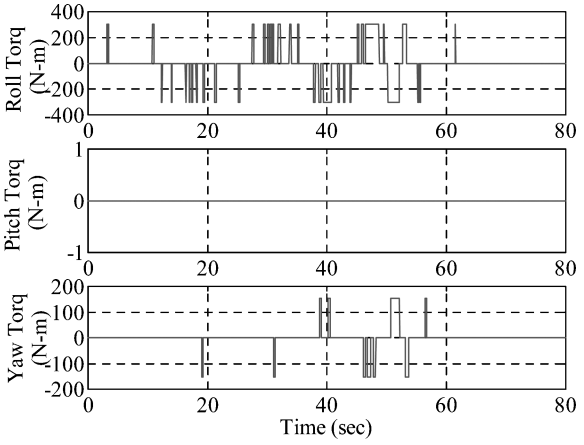

Fig. 10 Six-DOF case study, reaction control system response.

As the trajectory crosses the original switching curves from the coast region to the firing region, the RCS jets are commanded on. If the phase-plane trajectory enters the region between the original switching curve and the adjacent hysteresis switching curve, the RCS jets are commanded to remain on until the trajectory crosses the corresponding hysteresis curve. The jets remain on for some time after the trajectory crosses the original switching curve, and thus the high-frequency jet cycling is reduced while the trajectory is steered towards the desired limit cycle. The width of the hysteresis region was reduced to zero by an amount proportional to the rate error as the rate error became lower than a threshold of about 7 deg/s. This shaping of the hysteresis region was used to drive the phase-plane trajectory toward the desired location at the termination of the switching curves at zero rate error. The shape of the hysteresis regions is somewhat arbitrary, and the candidate switching curves definitions were chosen to provide good command tracking while reducing chattering and fuel usage for the MSL application.

The time responses in Figs. 9 and 10 demonstrate the improved controller behavior. Figure 9 shows the vehicle angle-of-attack, sideslip, and bank-angle responses. The aerodynamics exhibit minimal damping in pitch and yaw; hence, the angle-of-attack and sideslip oscillatory response about the aerodynamic trim conditions. The bank-angle response follows the guidance command with good performance indicated by minimal command response lag and overshoot. Figure 10 shows the RCS torque command demonstrating significant reduction in the high-frequency chattering. Figure 8 shows the phase-plane plot for the six-DOF case study along with the complete set of switching curves for the modified controller.

Conclusions

A phase-plane controller based on the reaction control system (RCS) controller used for the Apollo command module digital

autopilot was used as an atmospheric entry controller for the Mars Science Laboratory (MSL) probe. Useful controller modifications for the MSL application have been presented in this paper. These include modification of the switching curves for the roll phase plane to provide improved response to bank reversals and the addition of hysteresis switching curves to prevent RCS chattering for high-frequency controller updates. Phase-plane methods for aerodynamic angle feedback were also presented for the purpose of providing improved angle-of-attack control and turn coordination at conditions of low dynamic pressure. Controller performance was demonstrated in a six-DOF simulation of the candidate entry vehicle configuration using no-wind estimates of the attitude from the navigation system.

References

[1]Miller, J. E. (ed.), "Part 7: Space Vehicle Flight Control," *Space Navigation Guidance and Control*, Technivision, Ltd., Maidenhead, England, U.K., 1966, pp. 329–370.

[2]Powell, R. W., Striepe, S. A., Desai, P. N., Tartabini, P. V., Queen, E. M., Brauer, G. L., Cornick, D. E., Olson, D. W., Petersen, F. M., Stevenson, R., Engle, M. C., and Marsh, S. M., "Program to Optimize Simulated Trajectories: Volume II, Utilization Manual," Ver. 1.1.1.G, Lockheed Martin Corp., May 2000.

[3]"Guidance System Operations Plan for Manned CM Earth Orbital and Lunar Missions Using Program Colossus 3, Sec. 3, Digital Autopilots (Rev. 14)," NASA Contract NAS 9-4065, MIT IL R-577, Cambridge, MA, March 1972.

[4]Mendeck, G. F., and Carman, G. L., "Guidance Design for Mars Smart Landers Using the Entry Terminal Point Controller," AIAA Paper 2002-4502, Aug. 2002.

[5]Justus, C. G., and James, B. F., "Mars Global Reference Atmosphere Model 2000 Version (Mars-GRAM 2000): User's Guide," NASA TM-2000-210279, May 2000.

[6]"Using Simulink," The Mathworks, Inc., Natick, MA, July 2002.

[7]"Using MATLAB," The Mathworks, Inc., Natick, MA, Nov. 2000.

[8]Striepe, S. A., Queen, E. M., Powell, R. W., Braun, R. D., Cheatwood, F. M., Aguirre, J. T., Sachi, L. A., and Lyons, D. T., "An Atmospheric Guidance Algorithm Testbed for Mars Surveyor Program 2001 Orbiter and Lander," AIAA Paper 98-4569, Aug. 1998.

[9]Bobskill, G. J., Parikh, P. C., Prabhu, R. K., and Tyler, E. D., "Aerodynamic Database Development for Mars Smart Lander Vehicle Configurations," *Journal of Spacecraft and Rockets*, Vol. 43, No. 2, 2006, pp. 303–310; also AIAA Paper 2002-4411, Aug. 2002.

[10]Crain, T. P., and Bishop, R. H., "Mars Entry Navigation: Atmospheric Interface Through Parachute Deploy," AIAA Paper 2002-4501, Aug. 2002.

M. K. Lockwood
Guest Editor

Color reproductions courtesy of NASA Langley Research Center.